Determination of the tungsten isotope composition in seawater: The first vertical profile from the western North Pacific Ocean

Yuta Fujiwara [a], Makoto Tsujisaka [a], Shotaro Takano [a], and Yoshiki Sohrin [a,*]

[a] Institute for Chemical Research, Kyoto University, Gokasho, Uji, Kyoto 611-0011, Japan

*Corresponding author.

E-mail address: sohrin@scl.kyoto-u.ac.jp (Y. Sohrin)

Phone number: 81-774-38-3100 (Y. Sohrin)

Abstract

The stable isotope ratio of W is a new tracer in oceanographic studies and a new proxy in paleoceanographic studies; however, precise data for modern seawater have not been reported to date. Because the concentration of W in seawater is as low as 49 pmol kg^{-1}, an ~3000-fold preconcentration is necessary prior to measurement by multicollector inductivity coupled plasma mass spectrometry (MC-ICP-MS). For the preconcentration, we investigated solid-phase extraction using chelating resins, namely, NOBIAS Chelate-PA1 with ethylenediaminetriacetic acid groups and TSK-8HQ with 8-hydroxyquinolie groups. We report that TSK-8HQ is useful because the effects of the seawater matrix are minor thermodynamically and kinetically. We present a novel method for analysis of the concentrations and isotope ratios of W and Mo in seawater, consisting of solid phase extraction, chromatographic separation using anion exchange resin AG1 X8, and measurement by MC-ICP-MS. Both W and Mo are quantitatively recovered by this method, which was applied to seawater samples collected from the North Pacific Ocean. The measured concentration of W and the concentration and isotope ratio of Mo are consistent with those in the literature. The isotope ratio of W is found to be uniform throughout the water column in

the western North Pacific Ocean; $\delta^{186/184}$W is 0.55 ± 0.12‰ (ave ± 2sd, *n* = 7) using NIST SRM 3163 as a reference for W. On the basis of this data, we determined that the isotopic difference in $\delta^{186/184}$W is ~0.49‰ between seawater and oxic sediments in the modern ocean. This value accords with the reported experimental data for the isotope fractionation of W during adsorption on manganese and iron (oxyhydr)oxides, suggesting the validity of our data.

Keywords: Tungsten isotope; Molybdenum isotope; Seawater; Chemical separation; MC-ICP-MS; North Pacific Ocean

1. Introduction

Stable isotope ratios of heavy metals are emerging as new tracers in oceanography and new proxies in paleoceanography owing to the development of analytical techniques using multicollector inductivity coupled plasma mass spectrometry (MC-ICP-MS) (Anbar and Rouxel, 2007; Boyle et al., 2012; Homoky et al., 2016). However, our knowledge on the distribution of stable isotope ratios of heavy metals in the modern ocean is still limited for certain elements, such as V (Wu et al., 2019), Cr (Moos and Boyle, 2019), Fe (Conway and John, 2014), Ni (Takano et al., 2017), Cu (Takano et al., 2014), Zn (Sieber et al., 2020), Ge (Guillermic et al., 2017), Mo (Nakagawa et al., 2012), Cd (Schmitt et al., 2009), Ba (Horner et al., 2015), Nd (Lacan et al., 2012), Hf (Zimmermann et al., 2009), and Pb (Zurbrick et al., 2018).

Tungsten and Mo are Group 6 elements. The upper crustal abundance of W is 1.9 ppm, which is close to that of Mo at 1.1 ppm (Rudnick and Gao, 2005). In oxic seawater, W and Mo dissolve as oxyanions WO_4^{2-} and MoO_4^{2-}, respectively; however, the concentration of W is 49 pmol kg^{-1}, which is 2000 times lower than that of Mo at 107 nmol kg^{-1} (Collier,

1985; Firdaus et al., 2008; Nakagawa et al., 2012; Sohrin et al., 1987). This difference is ascribed to the fact that the sinks for W and Mo in the oxic ocean are Mn and Fe (oxyhydr)oxides (Shimmield and Price, 1986) and that the distribution ratio of W between the (oxyhydr)oxides and seawater is several hundred times higher than that of Mo (Kashiwabara et al., 2017; Kashiwabara et al., 2013; Kashiwabara et al., 2011; Sohrin et al., 1987). In sulfidic seawater, MoO_4^{2-} is transformed into particle-reactive thiomolybdate anions $MoO_xS_{4-x}^{2-}$ ($0 \leq x \leq 3$) and removed from solution at a H_2S concentration above 11 μmol kg^{-1} (Erickson and Helz, 2000). However, thiotungstate is formed at a H_2S concentration above 60 μmol kg^{-1} and is not particle reactive (Mohajerin et al., 2016), resulting in W enrichment in anoxic hydrothermal fluids (Kishida et al., 2004). Recently, a laboratory experiment has shown that WO_4^{2-} converts to WS_4^{2-} around 1.0 mmol kg^{-1} H_2S at equilibrium (Cui et al., 2020). This substantial fractionation of W and Mo in the hydrosphere is quite unique among twin elements in the same group. Tungsten has five stable isotopes: ^{180}W (natural abundance 0.12%), ^{182}W (26.50%), ^{183}W (14.31%), ^{184}W (30.64%), and ^{186}W (28.43%) (de Laeter et al., 2003). Molybdenum has seven stable isotopes: ^{92}Mo (14.77%), ^{94}Mo (9.23%), ^{95}Mo (15.90%), ^{96}Mo (16.68%), ^{97}Mo (9.56%), ^{98}Mo (24.19%), and ^{100}Mo (9.67%) (de Laeter et al., 2003). Although Mo stable isotopes have been actively studied, especially as proxies for redox conditions in paleoceanography (Nägler et al., 2011; Neubert et al., 2008; Ostrander et al., 2019; Scholz et al., 2018; Thoby et al., 2019; Wang et al., 2019), the study of W stable isotopes is still in the early stages. Several studies reported analytical methods and data of geological reference materials for W (Abraham et al., 2015; Breton and Quitte, 2014; Krabbe et al., 2017; Kurzweil et al., 2018; Tsujisaka et al., 2019; Zhang et al., 2019). Only a few studies reported stable W isotope data for geological samples (Kurzweil et al., 2019; Kurzweil et al., 2020; Mazza et al., 2020).

To the best of our knowledge, stable isotope data for dissolved W in seawater have

not been reported to date. High precision is necessary to detect isotope fractionation for such a heavy element. For precise determination by MC-ICP-MS, W in seawater should be preconcentrated more than one thousand-fold and separated from coexisting elements. Additionally, the recovery of W through chemical separation should be quantitative to avoid an isotope fractionation. In previous studies, we developed precise analytical methods to determine isotopic ratios of Mo in seawater (Nakagawa et al., 2008) and those of W and Mo in sediments (Tsujisaka et al., 2019). In this study, we compare chelating resins, namely, NOBIAS Chelate-PA1 with ethylenediaminetriacetic acid groups and TSK-8HQ with 8-hydroxyquinolie groups, for preconcentration of W from a large volume of seawater. Then, we present a novel analytical method for determining the isotopic ratios of W in seawater. Finally, we report the first vertical profile of the isotopic ratio of W in the western North Pacific Ocean and the first estimate of isotopic difference in $\delta^{186/184}$W between seawater and oxic sediments in the ocean.

2. Material and methods

2.1. Reagents and materials

Reagent-grade HCl, HF, HNO_3, H_2SO_4, H_2O_2, NH_3, and tetramethylammonium hydroxide (TMAH) (FUJIFILM Wako Pure Chemical, Japan) were used for material cleaning and analysis. Metal standard solutions (FUJIFILM Wako Pure Chemical) were used to prepare working standard solutions for concentration measurements. NIST SRM 3163 and 3134 standards (National Institute of Standards and Technology, USA) were used as the isotopic standards for W and Mo, respectively (Irisawa and Hirata, 2006; Nägler et al., 2014). Standard solutions of Re (FUJIFILM Wako Pure Chemical) and Ru (Thermo Fisher Scientific, USA) were diluted and added to sample solutions as external element correction for W and Mo, respectively. Ultrapure water prepared with a Milli-Q Integral MT system (Merck

Millipore, Germany) was used throughout the experiments.

Seawater samples and all solutions were stored in low-density polyethylene (LDPE) containers (SEKISUI SEIKEI, Japan) or bottles (Nalge Nunc Int., USA). Perfluoroalkoxy alkane (PFA) vials (Savillex, USA) were used for sample digestion. These bottles and vials were cleaned as follows: first, they were soaked in an alkaline detergent solution of ~5% Scat 20X-PF (Nacalai Tesque, Japan) overnight and rinsed with tap water and Milli-Q water, and then, they were soaked in 3 M HCl overnight and rinsed with Milli-Q water. Finally, the bottles were soaked in 2 M NH_3 overnight and rinsed with Milli-Q water. Other materials, such as micropipette tips, columns, and tubes, were cleaned in a similar manner.

We prepared TSK-8HQ in accordance with methods used in previous studies (Dierssen et al., 2001; Firdaus et al., 2007). The 8HQ group was immobilized onto vinyl polymer resin via a single step synthesis; 6.0 g 5-amino-8-hydroxyquinoline dihydrochloride (Tokyo Kasei Kogyo, Japan) and 3.0 g Toyopearl AF-Epoxy-650M (40–90 μm bead size; Tosoh, Japan) were mixed in ~40 mL of aqueous solution at pH 11.5 in a PFA bottle and shaken at 45°C for 6 h using a constant temperature incubator shaker (TAITEC, Japan). The previous trade name of Toyopearl was TSK-Gel, which was incorporated into the name of TSK-8HQ according to previous studies (Dierssen et al., 2001; Firdaus et al., 2007). The TSK-8HQ resin was sieved with a Teflon screen of 230 mesh to remove small particles. The TSK-8HQ resin was cleaned by passing 50 mL 0.5 M NaOH, 75 mL ultrapure water, 50 mL 1.0 M HCl, and 75 mL ultrapure water, successively. This cleaning procedure was repeated until the filtrate became colorless. The cleaned TSK-8HQ resin was kept in ultrapure water in a LDPE bottle. The TSK-8HQ resin (~200 mg dry weight) was packed in an empty cartridge (Type L, TOMOE, Japan), of which the body was polypropylene, frits were polyethylene, inner diameter was 12 mm, and bed height was 6.5 mm.

The other chelating resin column used in this study was Nobias Chelate-PA-1W

(Hitachi High-Technologies, Japan). In the column, approximately 600 mg of the resin was sandwiched between frits of high-density polyethylene and sealed in a cartridge of polypropylene. Prior to use, the column was successively cleaned with 100 mL each of acetone (reagent grade), ultrapure water, 3 M HNO_3, ultrapure water, 2 M NH_3, and ultrapure water by injecting the solutions at a flow rate of ~5 mL min^{-1} using a polypropylene syringe.

Anion exchange resin AG1 X8 (200–400 mesh, Bio Rad, USA) was used to separate W and Mo from the remaining matrix elements. The resin was soaked in 1 M HNO_3 in a PFA bottle and shaken for 30 min. Then, the acid solution was replaced with a new solution. After five repetitions of this cleaning method, the resin was rinsed with ultrapure water. A polypropylene column (Muromac Mini-column S, Muromachi Chemicals, Japan) was charged with ~0.4 g AG1 X8 resin (5 mm internal diameter and 30 mm bed height).

2.2. Seawater samples

Seawater samples were collected from the Pacific Ocean using a clean sampling system (Sohrin and Bruland, 2011) during the cruises of R/V Hakuho Maru, JASMSTEC. The seawater samples collected in sampling bottles were filtered through an AcroPak capsule filter with a pore size of 0.2 μm (Pall, USA), collected in a precleaned 5 L LDPE container, added with HCl (Ultrapur-100, Kanto Chemical, Japan) to a final concentration of 0.01 M, and stored at an ambient temperature. For method-development experiments, seawater samples were mixed in a precleaned 60 L polypropylene tank (Nalge Nunc Int.). For analysis of vertical profiles, seawater samples were collected from several depths at station CL-2 (47°00'N, 160°00'E; bottom depth of 5195 m; sampling depths from 10–5186 m with an interval of approximately 500 m) in the western North Pacific Ocean during the KH-17-3 cruise in June 2017.

2.3. Chemical separation

2.3.1. Solid-phase extraction using chelating resin

Two serial-coupled columns of TSK-8HQ were used for seawater analysis. The preconcentration system (Fig. 1) was constructed with chelating resin columns, PFA tubes with a 2 mm internal diameter, PharMed tubes (06508-14, SAINT-GOBAIN, France) with a 1.6 mm internal diameter, Tygon tubes (LMT-55, SAINT-GOBAIN) with a 4 mm internal diameter, and a Masterflex pump (7520-40, Cole-Parmer, USA). Every step of the chemical analysis was carried out in a clean hood. First, the chelating resin columns were cleaned by passing 100 mL each of 3 M HNO_3, ultrapure water, 2 M NH_3, and ultrapure water. The flow rates of the solutions were maintained at 4 mL min^{-1}. Then, the columns were conditioned using a flow of 50 mL 0.04 M HCl (pH 1.4). Approximately 3 kg of the seawater sample was adjusted to pH 1.4 with HCl and then introduced into the columns. Finally, 70 mL 0.04 M HCl (pH 1.4) was passed through the columns to remove remaining matrix elements from the columns.

The chelating resin columns were detached from the preconcentration system and connected with a polypropylene syringe for elution of the elements. An eluate of 40 mL 5 M HF was passed through the columns in the direction opposite to that for sample loading by gravity flow at a flow rate of 0.3 mL min^{-1}. The eluates were collected in PFA vials. The chelating resin columns were again mounted to the preconcentration system and cleaned with 125 mL ultrapure water for the next use. One cycle of the solid-phase extraction took approximately 15 h to complete.

The eluate in a PFA vial was heated to dryness at 160°C on a hot plate (Analab, France). The residual organic matter from the chelating resin was decomposed by adding 2 mL 13 M HNO_3, 0.2 mL 10 M H_2O_2, and 0.1 mL 0.3 M H_2SO_4; capping the vial loosely; and heating the sample at 160°C for 8 h. The sample was then uncapped, heated to near dryness,

and redissolved in a 2 mL mixture of 0.5 M HF and 0.4 M HCl by heating at 80°C for 3 h.

2.3.2. Anion exchange separation

Chromatographic separation using anion exchange resin AG1 X8 was applied to the preconcentrated sample to separate W and Mo from the remaining matrix elements. The procedure was in accordance with that of our previous study (Tsujisaka et al., 2019). Every solution was sent through the column by gravity at a flow rate of 0.15 mL min^{-1}. The column was first cleaned by flowing 4 mL 6 M HNO_3 three times, 3 mL ultrapure water, and 1 mL 0.5 M HF–0.4 M HCl three times. The sample solution that has been preconcentrated was then loaded onto the resin. Matrix elements, such as Fe and Mn, were eluted using a flow of 1 mL 1 M HF three times. Subsequently, high field strength elements, such as Ti, Zr, and Hf, were eluted using a flow of 1 mL 0.05 M HF–9 M HCl three times. Tungsten was eluted using 3 mL 5 M HCl five times and collected in a PFA vial. Molybdenum was finally eluted using 3 mL 1 M HNO_3 three times and collected in another PFA vial. One cycle of anion exchange separation took approximately 5 h to complete.

The purified solutions of Mo and W were evaporated at 160°C on a hot plate. The residual organic materials from the anion exchange resin were decomposed in a manner similar to that in the last section but without addition of H_2SO_4. After evaporation of the acids, the residues were redissolved with 1.2 g 0.0055 M TMAH for W and 20 g 0.15 M HNO_3 for Mo by heating at ~80°C for 3 h. An accurate concentration factor was calculated on a weight basis.

2.4. Measurement of element concentrations and isotope ratios

The element concentrations were determined by a calibration curve method using a NexION 350D quadrupole ICP mass spectrometer (Perkin Elmer, USA). The isotopic

compositions of W and Mo were measured using a Neptune Plus MC-ICP mass spectrometer (Thermo Fisher Scientific) at the Research Institute for Humanity and Nature (RIHN), Japan. The measurements were in accordance with those in a previous study (Tsujisaka et al., 2019). Seven faraday cups were used for W: L3 (^{182}W), L2 (^{183}W), L2 (^{184}W + ^{184}Os), C (^{185}Re), H1 (^{186}W + ^{186}Os), H2 (^{187}Re + ^{187}Os), and H3 (^{188}Os). The isotope ^{180}W was not monitored in this study because of its low natural abundance (0.12%). Isobaric isotopes of ^{184}Os, ^{186}Os, and ^{187}Os on ^{184}W, ^{186}W, and ^{187}Re were corrected by monitoring ^{188}Os. Then, the instrumental mass bias was corrected by standard-sample bracketing combined with external mass bias correction using Re. The isotope ratio of W is presented as a delta value (‰) relative to that of the NIST SRM 3163 standard (Irisawa and Hirata, 2006):

$$\delta^{186/184}\mathrm{W} = \left(\frac{\left(^{186}\mathrm{W}/^{184}\mathrm{W}\right)_{\mathrm{sample}}}{\left(^{186}\mathrm{W}/^{184}\mathrm{W}\right)_{\mathrm{NIST\ SRM\ 3163}}} - 1 \right) \times 1000 \quad (1)$$

Nine faraday cups were used for Mo: L4 (^{91}Zr), L3 (^{92}Mo + ^{92}Zr), L2 (^{94}Mo + ^{94}Zr), L1 (^{95}Mo), C (^{97}Mo), H1 (^{98}Mo + ^{98}Ru), H2 (^{99}Ru), H3 (^{101}Ru), and H4 (^{102}Ru). Isobaric interferences from ^{92}Zr and ^{94}Zr on ^{92}Mo and ^{94}Mo were corrected by monitoring ^{91}Zr. Then, the instrumental mass bias was corrected by standard-sample bracketing combined with external mass bias correction using Ru. The isotope ratio of Mo is presented as a delta value (‰) relative to that of the NIST SRM 3134 standard with a correction of +0.25‰ for easy comparison with the literature (Nägler et al., 2014):

$$\delta^{98/95}\mathrm{Mo} = \left(\frac{\left(^{98}\mathrm{Mo}/^{95}\mathrm{Mo}\right)_{\mathrm{sample}}}{\left(^{98}\mathrm{Mo}/^{95}\mathrm{Mo}\right)_{\mathrm{NIST\ SRM\ 3134}}} - 1 \right) \times 1000 + 0.25 \quad (2)$$

In this study, $\delta^{98/95}$Mo was not directly measured because ^{98}Mo has an isobaric isotope (^{98}Ru). We measured $\delta^{97/95}$Mo and converted the value to $\delta^{98/95}$Mo via multiplication by a factor of 3/2 based on mass-dependent fractionation. The concentrations of W and Mo were also calculated by using Re and Ru, respectively, as internal standards. The long-term instrumental reproducibility was evaluated using repeated measurements of the NIST SRM

3163 (W) and NIST SRM 3134 (Mo) standard solutions over a nine-month period; the average and 2 standard deviation was $\delta^{186/184}W = 0.00 \pm 0.02‰$ (n = 82) and $\delta^{98/95}Mo = 0.00 \pm 0.04‰$ (n = 94) (Tsujisaka et al., 2019).

3. Results and discussion

3.1. Comparison of chelating resins

3.1.1. Optimizing pH for NOBIAS Chelate-PA1 and TSK-8HQ columns

The dependency of recovery (%) of W on pH was investigated for chelating resins NOBIAS Chelate-PA1 and TSK-8HQ by column extraction using a single column. For NOBIAS Chelate-PA1, the sample solution was 500 g Milli-Q water with 500 pmol kg^{-1} W. The pH was adjusted with HNO_3 below pH 2.5 and ammonium acetate buffer above pH 2.5. The flow rate of the sample solution was 5 mL min^{-1}. For TSK-8HQ, the sample solution was 100 g mixed seawater with 20 nmol kg^{-1} W. The pH was adjusted with HCl below pH 2.2 and ammonium acetate buffer above pH 2.6. The flow rate of the sample solution was 9 mL min^{-1}. The results are presented in Fig. 2. For NOBIAS Chelate-PA1, the recovery was ~100% between pH 1.4 and pH 5.0. However, we found that a small amount of W passed through the column at pH 1.7–3.5. Thus, the optimum pH is 4.7. For TSK-8HQ, the recovery was highest at pH 1.2 and gradually decreased with increasing pH. Because the added amount of HCl is two times larger at pH 1.2 than at pH 1.4, we adopted 1.4 as the optimum pH to reduce the amount of HCl.

3.1.2. Adsorption capacity for each resin

The adsorption capacity (mol g^{-1}) is defined as the maximum amount of an element adsorbed on a unit dry weight of chelating resin. The adsorption capacity of W on NOBIAS Chelate-PA1 and TSK-8HQ was investigated via batch experiments. For NOBIAS

Chelate-PA1, the sample solutions were Milli-Q water and mixed seawater adjusted to pH 4.7 with 50 mM ammonium acetate buffer. For TSK-8HQ, the sample solutions were Milli-Q water and mixed seawater adjusted to pH 1.4 with HCl. A 100 g sample solution with 325 μmol kg^{-1} W and a chelating resin of 0.01 g in dry weight were shaken at 25°C for 2 h using a constant temperature incubator shaker. Then, the equilibrium concentration of W in solution was determined by ICP-MS after dilution to calculate the adsorption capacity. The results are listed in Table 1. There is no significant difference for each resin between the capacities in Milli-Q water and mixed seawater. The capacity of TSK-8HQ is approximately two times higher than that of NOBIAS Chelate-PA1. The adsorption capacity of W in seawater per column is 0.43 mmol for NOBIAS Chelate-PA1 (with ~600 mg resin) and 0.29 mmol for TSK-8HQ (with ~200 mg resin). Assuming that the capacity of Mo is as high as that of W, these values are 1000 times the amount of Mo in 3 kg of seawater. Thus, a single column of NOBIAS Chelate-PA1 and TSK-8HQ has enough capacity for quantitative recovery of W and Mo from seawater.

3.1.3. Distribution coefficient for each resin

The distribution coefficient (D) is defined by the following equation:

$$D = \frac{C_{\text{solid}}}{C_{\text{solution}}} \quad (3)$$

where C_{solid} and C_{solution} represent the concentration (mol kg^{-1}) in solid and solution phases, respectively. We measured D of W for the chelating resins in Milli-Q water and mixed seawater in a manner similar to that of the adsorption capacity but changing the initial concentration of W. The adsorption capacity was measured at a high concentration of W to determine the maximum amount of W that was complexed with the resin. The distribution coefficient was measured to determine a thermodynamic parameter at a low concentration of W that was used for practical preconcentration. The value of D substantially increased as the

initial concentration of W decreased (Fig. 3). The results for 5.5 μmol kg^{-1} W in the initial concentration are listed in Table 1. The values of *D* are significantly higher in Milli-Q water than in mixed seawater for both the chelating resins; the difference is much higher for NOBIAS Chelate-PA1 than for TSK-8HQ. These results suggest that the major components in seawater interfere with the surface complexation of W on the chelating resins at equilibrium, and the interference is more severe for NOBIAS Chelate-PA1 than for TSK-8HQ.

3.1.4. Comparison of columns for W recovery

The recovery of W from a large volume of solution was investigated via column extraction. For NOBIAS Chelate-PA1, 6 kg Milli-Q water with 500 pmol kg^{-1} W was adjusted to pH 4.7 and was passed through a column at a flow rate of 5 mL min^{-1}. The recovery of W was 93–107% (n = 2). We found, however, that this condition is not sufficient to recover W from seawater. Five kg of mixed seawater containing 50 pmol kg^{-1} W and adjusted to pH 4.7 was passed through 6 serial-coupled columns of NOBIAS Chelate-PA1 at a flow rate of 1 mL min^{-1}. The recovery of W by each column is shown in Fig. 4. The results are best fitted by the following exponential curve:

$$y = 116.6\exp(-0.732x) \qquad (r^2 = 0.958,\ n = 6) \qquad (4)$$

where y represents recovery (%) of each column and x represents the number of the xth column. The results indicate that 6 serial-coupled columns of NOBIAS Chelate-PA1 and a slow flow rate are necessary to recover a sufficient amount of W from seawater.

For TSK-8HQ, 5 kg Milli-Q water added with 200 pmol kg^{-1} W and 100 nmol kg^{-1} Mo and adjusted to pH 1.4 was passed through 2 serial-coupled columns at a flow rate of 8 mL min^{-1}. The recovery of W was 106 ± 8% (ave ± 2sd; n = 6), and that of Mo was 94 ± 10% (n = 6). Three kilograms of mixed seawater containing 50 pmol kg^{-1} W and adjusted to pH 1.4 was passed through 2 serial-coupled columns at a flow rate of 4 mL min^{-1}. The recovery of W

by each column is shown in Fig. 4. The results are best fitted by the following exponential curve:

$$y = 420.6\exp(-1.62x) \qquad (n = 2) \qquad (5)$$

The results indicate that 2 serial-coupled columns of TSK-8HQ are sufficient to recover an adequate amount of W from seawater. To confirm this conclusion, 5 kg mixed seawater with and without spiking of 37 pmol kg^{-1} W adjusted to pH 1.4 was passed through 2 serial-coupled columns at a flow rate of 8 mL min^{-1}. The recovery from the solution spiked with W was 98–108% (n = 2). In addition, the concentration of Mo was 105 ± 18 nmol kg^{-1} (n = 4), which is consistent with the reported average concentration of Mo in seawater, implying quantitative recovery of Mo.

These results suggest that the major components in seawater strongly interfere with the surface complexation of W on NOBIAS Chelate-PA1 kinetically as well as thermodynamically. Thus, we decided to use 2 serial-coupled columns of TSK-8HQ for preconcentration of W from seawater. A disadvantage of TSK-8HQ is gradual dissociation of 8HQ groups during usage. However, the 2 serial-coupled columns did not show a significant deterioration in efficiency after five cycles of the preconcentration procedure for 3 kg seawater.

3.2. Optimization of the analytical procedure for seawater

We first used a HNO_3 solution to elute W and Mo from TSK-8HQ, but the recovery was not sufficient. A sufficient elution was attained by flowing a HNO_3 solution, Milli-Q water, and a NH_3 solution successively. In this case, each eluate has to be collected separately, and W in each eluate has to be combined after evaporation of the eluents to prevent remnant NH_4NO_3. To avoid this, we instead used 5 M HF as the eluent, because we determined that W and Mo were quantitatively recovered with only 5 M HF.

Eluates from the columns of TSK-8HQ and AG1 X8 contained organic matter, which interfere with measurement by ICP-MS. Thus, acid decomposition of organic matter in the eluates was necessary. When we used HNO_3–H_2O_2 for decomposition, evaporated the acids to dryness, and redissolved W in 0.4 M HCl, the recovery was 82–84% (n = 2). This result is probably caused by the formation of passive-state W oxides. To prevent this issue, we added a small amount of H_2SO_4 to keep W in small drops of H_2SO_4 solution after the evaporation of HNO_3–H_2O_2 in a manner similar to that adopted for the determination of Zr, Nb, Hf, and Ta (Tanaka et al., 2019). When 0.1 mL 0.3 M H_2SO_4 was added to HNO_3–H_2O_2, the recovery of W was 98–102% (n = 2). Because W was highly soluble in the TMAH solution, H_2SO_4 was not added to decompose the eluate from AG1 X8. In addition, H_2SO_4 was not added to decompose the eluate of Mo from AG1 X8, since Mo was readily redissolved in the HNO_3 solution.

Hence, we established the optimum procedure for seawater analysis, by which W is concentrated from 3 kg seawater to 1.2 g 0.0055 M TMAH, as described in the method section. The whole chemical separation procedure takes approximately 50 h. Samples of Milli-Q water added with the NIST SRM 3163 standard to a final concentration of 259 pmol kg^{-1} were analyzed by this optimum procedure. The recovery of W was 99–100% (n = 2), and $\delta^{186/184}W$ was 0.025–0.035‰ (n = 2). These results confirm that the recovery of W is quantitative and that the mass fractionation of W during the procedure is negligible.

Samples of mixed seawater with and without spiking of the W isotope standard to a final spike concentration of 54 pmol kg^{-1} were also analyzed using this optimum procedure. The recovery of W from the spiked seawater was 89–106% (n = 2). $\delta^{186/184}W$ of the unspiked seawater was 0.47–0.53‰ (n = 2). $\delta^{186/184}W$ is plotted against the inverse W concentration in Fig. 5. The linear regression line has an intercept close to the origin, again suggesting that there is no significant mass fractionation of W during the procedure.

To investigate the reagent blank, we evaporated each reagent used in the optimized procedure, redissolved the residue in TMAH, and measured the concentration of W by ICP-MS. We found that the total reagent blank was 5.2×10^{-10} g W, which is 1.9% of the amount of W in 3 kg seawater.

The optimized procedure was applied to 5 kg seawater, and the amounts of coexisting elements (Ms) in the W and Mo fractions were investigated. The results are listed in Table 2. The M/W mole ratio is less than 18, and the M/Mo ratio is less than 5×10^{-3}, indicating that this procedure is efficient for separating W and Mo from coexisting elements in seawater.

3.3. Vertical profiles in the western North Pacific Ocean

The analytical results of seawater samples collected at station CL-2 (47°00'N, 160°00'E; bottom depth of 5195 m) are listed in Table 3. The vertical profiles of $\delta^{186/184}$W and $\delta^{98/95}$Mo are shown in Fig. 6. The concentrations and isotopic ratios of W and Mo are uniform from the surface to the bottom. The concentrations of W and Mo normalized to a salinity of 35 are 53 ± 4 pmol kg^{-1} (ave ± 2sd, n = 7) and 104 ± 6 nmol kg^{-1} (n = 10), respectively, for samples throughout the water column. $\delta^{98/95}$Mo is 2.37 ± 0.02‰ (n = 10). These values are consistent with the reported values in the literature (Firdaus et al., 2008; Nakagawa et al., 2012). The relative standard deviations for these values are 0.4–3.7%. $\delta^{186/184}$W in seawater is 0.55 ± 0.12‰ (n = 7), of which relative standard deviation is 11%. The uniform concentration of W in the modern ocean has been shown in previous studies (Firdaus et al., 2007; Sohrin et al., 1987). The data in this study suggest that the stable isotope composition of W is also uniform in the modern ocean as a first approximation. At present, we think the relatively high variations in $\delta^{186/184}$W are caused by analytical errors.

Assuming W is uniform throughout the water column, the average $\delta^{m/184}$W values for

all samples at station CL-2 are plotted against the mass number (m) of the W stable isotopes in Fig. 7. All points are located on a straight line passing through the coordinate (184, 0), suggesting that W in the ocean follows mass-dependent isotope effects and that there is no significant interference for any measured isotopes. The $\delta^{m/95}$Mo vs m plot also shows a straight line passing through the coordinate (95, 0), confirming the validity of estimating $\delta^{98/95}$Mo from $\delta^{97/95}$Mo on the basis of mass-dependent fractionation.

The vertical profile of $\delta^{186/184}$W in seawater is reported here for the first time as far as we know. To assess the accuracy of $\delta^{186/184}$W in seawater, we compared it with literature data for δ^{186}W in manganese nodules and oxic marine sediments (Fig. 8). Tungsten is highly enriched in hydrothermal fluids (Kishida et al., 2004). It is possible that also $\delta^{186/184}$W is affected by hydrothermal activity. Here we focus on the fractionation of W isotopes during adsorption from modern oxic seawater. Thus, we do not include the data for samples that were collected from a deep depth of a sediment core and from near hydrothermal sites and volcanoes. As shown in Fig. 8, $\delta^{186/184}$W in seawater is significantly higher than $\delta^{186/184}$W in manganese nodules and oxic sediments. Although there are moderate variations in $\delta^{186/184}$W in manganese nodules and oxic sediments, the difference in average $\delta^{186/184}$W between seawater and the solid phase is 0.49 ± 0.16‰. Similarly, the difference in average $\delta^{98/95}$Mo between seawater and the solid phase is 2.39 ± 0.86‰. Manganese nodules and oxic sediments are assumed to be major sinks of W and Mo in the oxic ocean (Sohrin et al., 1987). Mass fractionation of W during adsorption ($\Delta^{186/184}$W) is defined as follows:

$$\Delta^{186/184}\mathrm{W} = \delta^{186/184}\mathrm{W}_{\mathrm{solution}} - \delta^{186/184}\mathrm{W}_{\mathrm{solid}} \quad (6)$$

The laboratory experimental data have been reported for mass fractionation of W during adsorption on Mn and Fe (oxyhydr)oxides (Kashiwabara et al., 2017). The authors used 0.70 M NaCl solution at pH 8 instead of seawater. $\Delta^{186/184}$W was 0.59 ± 0.14‰ for ferrihydrite and

0.51 ± 0.06‰ for δ-MnO_2. Mass fractionation of Mo has been reported as follows: $\Delta^{98/95}$Mo is 1.0–1.3‰ for ferrihydrite (Goldberg et al., 2009) and 2.4–2.9‰ for δ-MnO_2 (Barling and Anbar, 2004). Thus, the observed differences in $\delta^{186/184}$W and $\delta^{98/95}$Mo between modern seawater and the manganese nodules and oxic sediments are comparable with the literature data of $\Delta^{186/184}$W and $\Delta^{98/95}$Mo, respectively. These results imply that both $\delta^{186/184}$W and $\delta^{98/95}$Mo in oxic seawater are generally controlled via adsorption on Mn and Fe (oxyhydr)oxides and that the $\delta^{186/184}$W values in this work are accurate.

4. Conclusions

A simple and precise analytical method has been developed to determine the concentration and isotopic ratio of W and Mo in seawater. A quantitative and ~3000-fold preconcentration of W is attained by column extraction using TSK-8HQ chelating resin. Thus, precise data for $\delta^{186/184}$W in seawater are presented here for the first time. This novel method and the data collected are expected to contribute to further development of the stable isotope marine chemistry and geochemistry of W.

The data in this study suggest that the stable isotope composition of W is uniform as well as the concentration of W in the modern ocean as a first approximation. Since the hydrothermal activity and anthropogenic contamination substantially increase the W concentration (Kishida et al., 2004; Sohrin et al., 1999), their effects on the isotope composition will be investigated in forthcoming studies. It is expected that the combination of the concentration and isotope composition would be useful to advance the marine geochemistry of W. In addition, the observed difference in $\delta^{186/184}$W between modern seawater and the manganese nodules and oxic sediments will be a useful constrain for paleoceanographic study.

Acknowledgements

The Neptune Plus MC-ICP-MS systems (Thermo Fisher Scientific) used in this study are joint-use facilities at the Research Institute for Humanity and Nature (RIHN), Japan. We would like to thank Ki-Cheol Shin for technical advice regarding measurements by MC-ICP-MS. We are grateful to Florian Kurzweil and two anonymous reviewers for constructive comments. In addition, we would like to extend our appreciation to graduate students Yusuke Nakagawa and Rena Murata, who performed the preliminary experiments of this study. This study was supported by a KAKENHI grant (grant number 19H01148) from the Japan Society for the Promotion of Science (JSPS) and a Research Grant for Environmental Isotope Study from the Research Institute for Humanity and Nature (grant number 19-59). We also thank Editage (www.editage.jp) for English language editing.

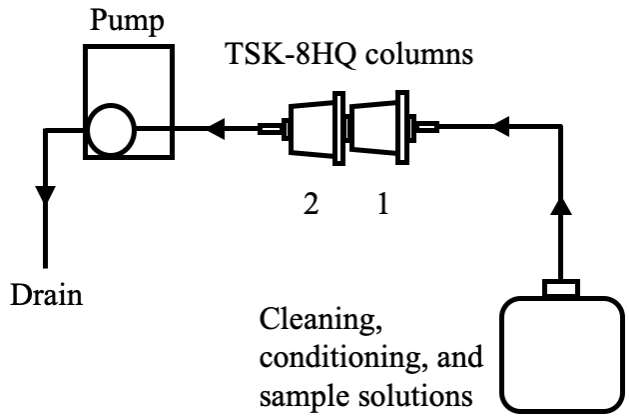

Fig. 1 Diagram of the preconcentration system with two serial-coupled columns of TSK-8HQ.

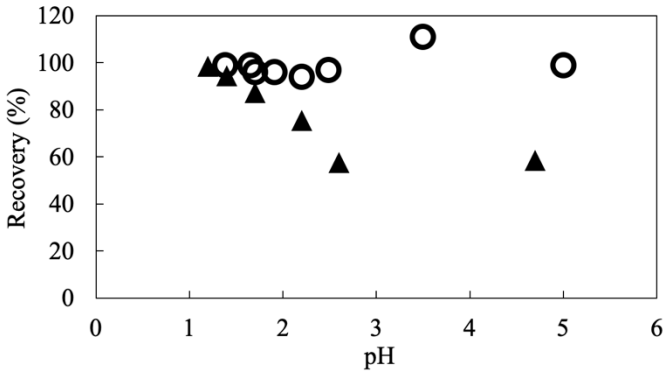

Fig. 2. pH dependence of the recovery (%) of W by column extraction using a single column. Open circles: NOBIAS Chelate-PA1. Closed triangles: TSK-8HQ. The sample solutions were Milli-Q water for NOBIAS Chelated-PA-1 experiments but seawater for TSK-8HQ experiments.

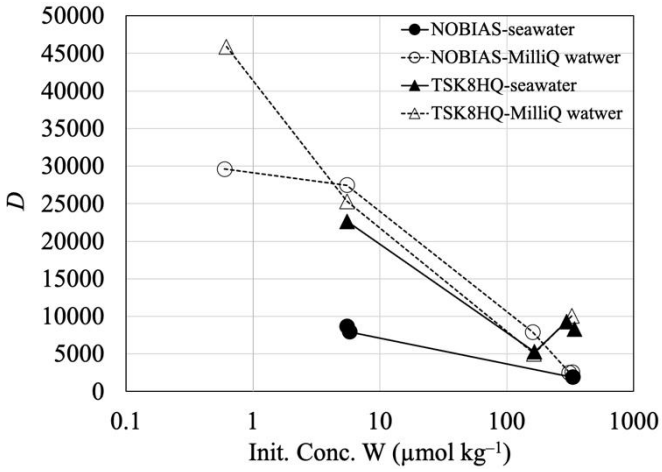

Fig. 3. Dependency of the distribution coefficient of W against the initial concentration of W in seawater or Milli-Q water. Solution pH was 4.7 for NOBIAS Chelate-PA1 and 1.4 for TSK-8HQ.

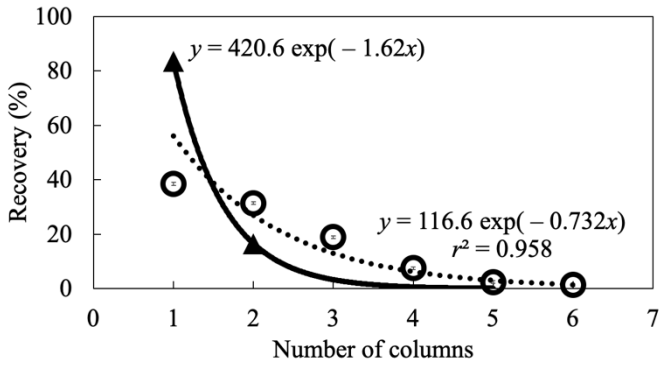

Fig. 4. Recovery (%) of W from seawater for each column via column extraction. Open circles: NOBIAS Chelate-PA1. Closed triangles: TSK-8HQ. The solid and dotted curves are calculated by curve fitting with exponential functions.

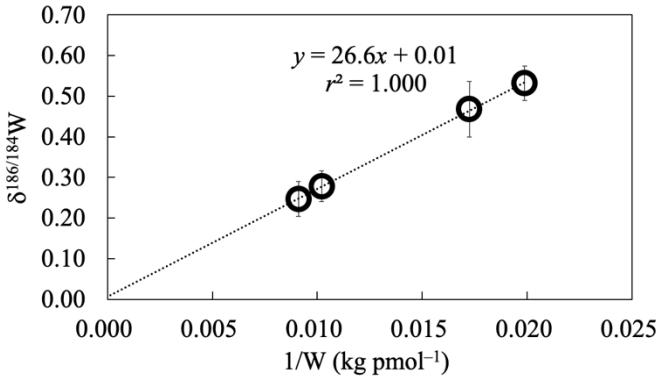

Fig. 5. $\delta^{186/184}$W vs the inverse W concentration for mixed seawater samples with and without spiking of the W isotope standard. The dotted line represents the linear regression. The error bars represent ±2 times the standard error of individual measurements.

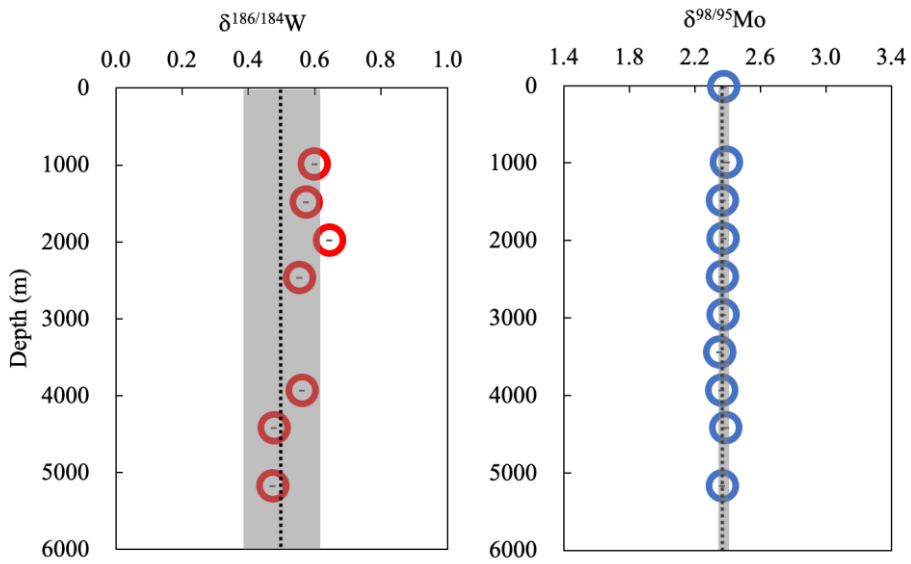

Fig. 6. Vertical profiles of isotopic ratios of W and Mo at station CL-2 (47°00'N, 160°00'E; bottom depth of 5195 m) in the western North Pacific Ocean. The error bars represent ±2 times the standard error of individual measurements. The dotted lines represent the averages throughout the water column, and the shaded areas represent ±2sd.

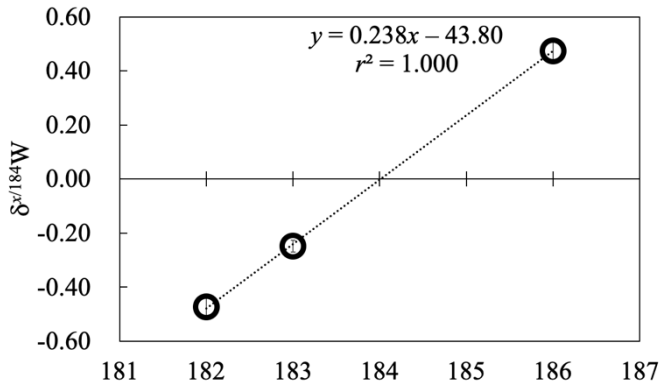

Fig. 7. $\delta^{m/184}$W vs the mass number (m) of W stable isotopes for the average of all samples collected from station CL-2. The error bars represent ±2sd. The dotted line represents the linear regression.

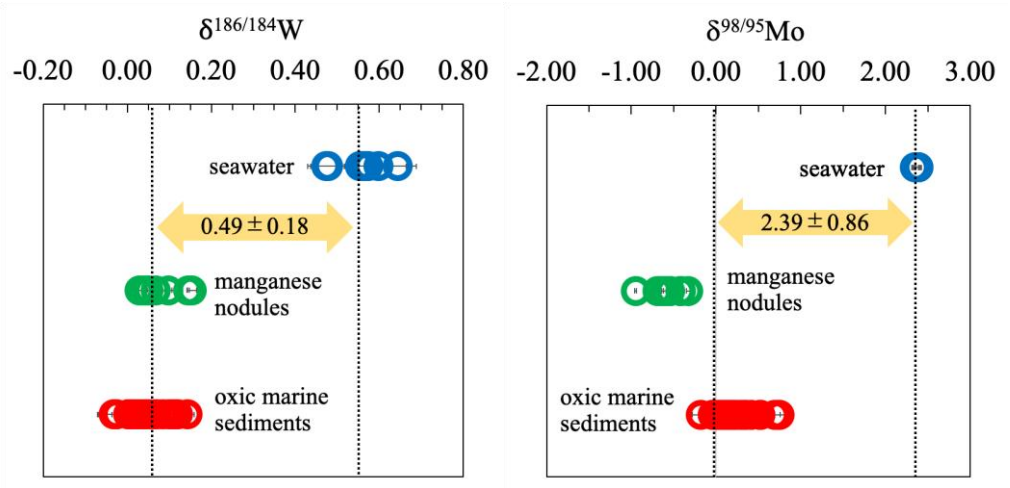

Fig. 8. $\delta^{186/184}W$ and $\delta^{98/95}Mo$ in seawater (this study) compared with those in manganese nodules (Abraham et al., 2015; Barling et al., 2001; Goto et al., 2015; Irisawa and Hirata, 2006; Kurzweil et al., 2019; Tsujisaka et al., 2019; Zhao et al., 2016) and oxic sediments from the Mediterranean Sea (Kurzweil et al., 2019) and the Japan Sea (Tsujisaka et al., in press). The error bars represent ±2 times the standard error of individual measurements. The dotted lines represent the averages for seawater and solid phases.

Table 1
Adsorption capacity and distribution ratio of W for NOBIAS Chelate-PA1 and TSK-8HQ.

Sample solution	Adsorption capacity (mmol g^{-1}; n = 2)		Distribution ratio (n = 2)	
	NOBIAS[a]	TSK-8HQ[b]	NOBIAS[c]	TSK-8HQ[d]
Milli-Q water	0.625–0.655	1.51–1.60	20689–34030	21884–28722
Seawater	0.525–0.895	1.43–1.52	8305–9014	20917–24408

[a] pH = 4.7.
[b] pH = 1.4.
[c] pH = 4.7, initial concentration of 5.5 μmol kg^{-1} W.
[d] pH = 1.4, initial concentration of 5.5 μmol kg^{-1} W.

Table 2

Coexisting elements in W and Mo fractions after chemical separation from 5 kg seawater.

		Na	Mg	K	Ca	Fe	Cu	Sr	Zr	Ru	Ba	Hf	Re	Os
W fraction (5 M HCl)	ng	105	28	2.6	154	11	1.8	0.9	5×10^{-2}	1.5	1.4	3×10^{-3}	9×10^{-3}	1×10^{-3}
	M/W mole ratio	18	4.6	0.26	15	0.81	0.12	4×10^{-2}	2×10^{-3}	6×10^{-2}	4×10^{-2}	6×10^{-5}	2×10^{-4}	2×10^{-5}
Mo fraction (1 M HNO_3)	ng	66	17	59	41	134	0.71	0.17	0.10	0.37	0.46	5×10^{-3}	5×10^{-2}	3×10^{-2}
	M/Mo mole ratio	5×10^{-3}	1×10^{-3}	3×10^{-3}	2×10^{-3}	4×10^{-3}	2×10^{-5}	4×10^{-6}	2×10^{-6}	7×10^{-6}	6×10^{-6}	5×10^{-8}	5×10^{-7}	3×10^{-7}

Table 3

Analytical data of seawater samples collected at station CL-2 (47°00'N, 160°00'E; bottom depth of 5195 m).

Depth (m)	Salinity	W (pmol kg^{-1})[a]	$\delta^{186/184}W$	2se[b]	Mo (nmol kg^{-1})[a]	$\delta^{98/95}Mo$	2se[c]
10	32.853				99.1	2.38	0.02
990	34.434	54.2	0.60	0.07	104.3	2.39	0.03
1481	34.434	53.0	0.57	0.05	108.6	2.37	0.03
1974	34.615	53.7	0.64	0.04	106.6	2.37	0.03
2465	34.649	52.2	0.55	0.04	104.3	2.37	0.03
2954	34.667	48.8	0.56	0.05	103.1	2.37	0.03
3443	34.806				107.2	2.35	0.04
3930	34.882				100.9	2.36	0.04
4417	34.690	54.7	0.48	0.04	105.8	2.39	0.03
5169	34.706	53.2	0.47	0.04	103.7	2.37	0.03
ave		52.8	0.55		104.4	2.37	
2sd		3.9	0.12		5.8	0.02	

[a] normalized to salinity = 35.

[b] standard error of $\delta^{186/184}W$.

[c] standard error of $\delta^{98/95}Mo$.

References

Abraham, K. et al., 2015. Determination of mass-dependent variations in tungsten stable isotope compositions of geological reference materials by double-spike and MC-ICPMS. J. Anal. At. Spectrom., 30(11), 2334-2342. https://doi.org/10.1039/C5JA00210A.

Anbar, A.D., Rouxel, O., 2007. Metal stable isotopes in paleoceanography. Annu. Rev. Earth Planet. Sci., 35(1), 717-746. https://doi.org/10.1146/annurev.earth.34.031405.125029.

Barling, J., Anbar, A.D., 2004. Molybdenum isotope fractionation during adsorption by manganese oxides. Earth Planet. Sci. Lett., 217(3-4), 315-329. https://doi.org/10.1016/s0012-821x(03)00608-3.

Barling, J., Arnold, G.L., Anbar, A.D., 2001. Natural mass-dependent variations in the isotopic composition of molybdenum. Earth Planet. Sci. Lett., 193(3-4), 447-457. https://doi.org/10.1016/s0012-821x(01)00514-3.

Boyle, E.A. et al., 2012. GEOTRACES IC1 (BATS) contamination-prone trace element isotopes Cd, Fe, Pb, Zn, Cu, and Mo intercalibration. Limnol. Oceanogr.: Methods, 10(9), 653-665. https://doi.org/10.4319/lom.2012.10.653.

Breton, T., Quitte, G., 2014. High-precision measurements of tungsten stable isotopes and application to earth sciences. J. Anal. At. Spectrom., 29(12), 2284-2293. https://doi.org/10.1039/C4JA00184B.

Collier, R.W., 1985. Molybdenum in the Northeast Pacific Ocean. Limnol. Oceanogr., 30(6), 1351-1354. https://doi.org/10.4319/lo.1985.30.6.1351.

Conway, T.M., John, S.G., 2014. Quantification of dissolved iron sources to the North Atlantic Ocean. Nature, 511(7508), 212-215. https://doi.org/10.1038/nature13482.

Cui, M., Mohajerin, T.J., Adebayo, S., Datta, S., Johannesson, K.H., 2020. Investigation of tungstate thiolation reaction kinetics and sedimentary molybdenum/tungsten enrichments: Implication for tungsten speciation in sulfidic waters and possible applications for paleoredox studies. Geochim. Cosmochim. Acta. https://doi.org/https://doi.org/10.1016/j.gca.2020.04.004.

de Laeter, J.R. et al., 2003. Atomic weights of the elements: Review 2000. Pure Appl. Chem., 75(6), 683-799. https://doi.org/10.1351/pac200375060683.

Dierssen, H., Balzer, W., Landing, W.M., 2001. Simplified synthesis of an 8-hydroxyquinoline chelating resin and a study of trace metal profiles from Jellyfish Lake, Palau. Mar. Chem., 73(3–4), 173-192. https://doi.org/10.1016/S0304-4203(00)00107-9.

Erickson, B.E., Helz, G.R., 2000. Molybdenum(VI) speciation in sulfidic waters: Stability and lability of thiomolybdates. Geochim. Cosmochim. Acta, 64(7), 1149-1158. https://doi.org/10.1016/s0016-7037(99)00423-8.

Firdaus, M.L., Norisuye, K., Nakagawa, Y., Nakatsuka, S., Sohrin, Y., 2008. Dissolved and labile particulate Zr, Hf, Nb, Ta, Mo and W in the western North Pacific Ocean. J. Oceanogr., 64(2), 247-257. https://doi.org/10.1007/s10872-008-0019-z.

Firdaus, M.L. et al., 2007. Preconcentration of Zr, Hf, Nb, Ta and W in seawater using solid-phase extraction on TSK-8-hydroxyquinoline resin and determination by inductively coupled plasma-mass spectrometry. Anal. Chim. Acta, 583(2), 296-302. https://doi.org/10.1016/j.aca.2006.10.033.

Goldberg, T., Archer, C., Vance, D., Poulton, S.W., 2009. Mo isotope fractionation during adsorption to Fe (oxyhydr)oxides. Geochim. Cosmochim. Acta, 73(21), 6502-6516. https://doi.org/10.1016/j.gca.2009.08.004.

Goto, K.T. et al., 2015. Molybdenum isotopes in hydrothermal manganese crust from the Ryukyu arc system: Implications for the source of molybdenum. Mar. Geol., 369, 91-99. https://doi.org/10.1016/j.margeo.2015.08.007.

Guillermic, M., Lalonde, S.V., Hendry, K.R., Rouxel, O.J., 2017. The isotope composition of inorganic germanium in seawater and deep sea sponges. Geochim. Cosmochim. Acta, 212, 99-118. https://doi.org/10.1016/j.gca.2017.06.011.

Homoky, W.B. et al., 2016. Quantifying trace element and isotope fluxes at the ocean–sediment boundary: a review. Philos. T. R. Soc. A, 374(2081), 20160246. https://doi.org/10.1098/rsta.2016.0246.

Horner, T.J., Kinsley, C.W., Nielsen, S.G., 2015. Barium-isotopic fractionation in seawater mediated by barite cycling and oceanic circulation. Earth Planet. Sci. Lett., 430, 511-522. https://doi.org/10.1016/j.epsl.2015.07.027.

Irisawa, K., Hirata, T., 2006. Tungsten isotopic analysis on six geochemical reference materials using multiple collector-ICP-mass spectrometry coupled with a rhenium-external correction technique. J. Anal. At. Spectrom., 21(12), 1387-1395. https://doi.org/10.1039/B607945H.

Kashiwabara, T. et al., 2017. Stable isotope fractionation of tungsten during adsorption on Fe and Mn (oxyhydr)oxides. Geochim. Cosmochim. Acta, 204, 52-67. https://doi.org/10.1016/j.gca.2017.01.031.

Kashiwabara, T. et al., 2013. Tungsten species in natural ferromanganese oxides related to its different behavior from molybdenum in oxic ocean. Geochim. Cosmochim. Acta, 106(0), 364-378. https://doi.org/10.1016/j.gca.2012.12.026.

Kashiwabara, T., Takahashi, Y., Tanimizu, M., Usui, A., 2011. Molecular-scale mechanisms of distribution and isotopic fractionation of molybdenum between seawater and ferromanganese oxides. Geochim. Cosmochim. Acta, 75(19), 5762-5784. https://doi.org/10.1016/j.gca.2011.07.022.

Kishida, K., Sohrin, Y., Okamura, K., Ishibashi, J.-i., 2004. Tungsten enriched in submarine hydrothermal fluids. Earth Planet. Sci. Lett., 222(3-4), 819-827. https://doi.org/10.1016/j.epsl.2004.03.034.

Krabbe, N., Kruijer, T.S., Kleine, T., 2017. Tungsten stable isotope compositions of terrestrial samples and meteorites determined by double spike MC-ICPMS. Chem. Geol., 450(Supplement C), 135-144. https://doi.org/10.1016/j.chemgeo.2016.12.024.

Kurzweil, F. et al., 2019. The stable tungsten isotope composition of modern igneous reservoirs. Geochim. Cosmochim. Acta, 251, 176-191. https://doi.org/10.1016/j.gca.2019.02.025.

Kurzweil, F., Münker, C., Hoffmann, J.E., Tusch, J., Schoenberg, R., 2020. Stable W isotope evidence for redistribution of homogeneous 182W anomalies in SW Greenland. Geochemical Perspectives Letters, 14, 53-57. https://doi.org/http://dx.doi.org/10.7185/geochemlet.2024.

Kurzweil, F., Münker, C., Tusch, J., Schoenberg, R., 2018. Accurate stable tungsten isotope measurements of natural samples using a 180W-183W double-spike. Chem. Geol., 476, 407-417. https://doi.org/10.1016/j.chemgeo.2017.11.037.

Lacan, F., Tachikawa, K., Jeandel, C., 2012. Neodymium isotopic composition of the oceans: A compilation of seawater data. Chem. Geol., 300-301(0), 177-184. https://doi.org/10.1016/j.chemgeo.2012.01.019.

Mazza, S.E., Stracke, A., Gill, J.B., Kimura, J.-I., Kleine, T., 2020. Tracing dehydration and melting of the subducted slab with tungsten isotopes in arc lavas. Earth Planet. Sci. Lett., 530, 115942. https://doi.org/10.1016/j.epsl.2019.115942.

Mohajerin, T.J., Helz, G.R., Johannesson, K.H., 2016. Tungsten–molybdenum fractionation in estuarine environments. Geochim. Cosmochim. Acta, 177, 105-119.

https://doi.org/10.1016/j.gca.2015.12.030.
Moos, S.B., Boyle, E.A., 2019. Determination of accurate and precise chromium isotope ratios in seawater samples by MC-ICP-MS illustrated by analysis of SAFe Station in the North Pacific Ocean. Chem. Geol., 511, 481-493. https://doi.org/10.1016/j.chemgeo.2018.07.027.
Nägler, T.F. et al., 2014. Proposal for an international molybdenum isotope measurement standard and data representation. Geostand. Geoanal. Res., 38(2), 149-151. https://doi.org/10.1111/j.1751-908X.2013.00275.x.
Nägler, T.F., Neubert, N., Böttcher, M.E., Dellwig, O., Schnetger, B., 2011. Molybdenum isotope fractionation in pelagic euxinia: Evidence from the modern Black and Baltic Seas. Chem. Geol., 289(1,Äì2), 1-11. https://doi.org/10.1016/j.chemgeo.2011.07.001.
Nakagawa, Y. et al., 2008. Precise isotopic analysis of Mo in seawater using multiple collector-inductively coupled mass spectrometry coupled with a chelating resin column preconcentration method. Anal. Chem., 80(23), 9213-9219. https://doi.org/10.1021/ac801383t.
Nakagawa, Y. et al., 2012. The molybdenum isotopic composition of the modern ocean. Geochem. J., 46(2), 131-141. https://doi.org/10.2343/geochemj.1.0158.
Neubert, N., Nägler, T.F., Böttcher, M.E., 2008. Sulfidity controls molybdenum isotope fractionation into euxinic sediments: Evidence from the modern Black Sea. Geology, 36(10), 775-778. https://doi.org/10.1130/g24959a.1.
Ostrander, C.M. et al., 2019. Multiple negative molybdenum isotope excursions in the Doushantuo Formation (South China) fingerprint complex redox-related processes in the Ediacaran Nanhua Basin. Geochim. Cosmochim. Acta, 261, 191-209. https://doi.org/10.1016/j.gca.2019.07.016.
Rudnick, R.L., Gao, S., 2005. Composition of the continental crust. In: Rudnick, R.L. (Ed.), The Crust. Treatise on Geochemistry. Elsevier-Pergamon, Oxford, pp. 1-64.
Schmitt, A.-D., Galer, S.J.G., Abouchami, W., 2009. Mass-dependent cadmium isotopic variations in nature with emphasis on the marine environment. Earth Planet. Sci. Lett., 277(1–2), 262-272. https://doi.org/10.1016/j.epsl.2008.10.025.
Scholz, F. et al., 2018. Sedimentary molybdenum cycling in the aftermath of seawater inflow to the intermittently euxinic Gotland Deep, Central Baltic Sea. Chem. Geol., 491, 27-38. https://doi.org/10.1016/j.chemgeo.2018.04.031.
Shimmield, G.B., Price, N.B., 1986. The behaviour of molybdenum and manganese during early sediment diagenesis -- offshore Baja California, Mexico. Mar. Chem., 19(3), 261-280. https://doi.org/10.1016/0304-4203(86)90027-7.
Sieber, M. et al., 2020. Cycling of zinc and its isotopes across multiple zones of the Southern Ocean: Insights from the Antarctic Circumnavigation Expedition. Geochim. Cosmochim. Acta, 268, 310-324. https://doi.org/10.1016/j.gca.2019.09.039.
Sohrin, Y., Bruland, K.W., 2011. Global status of trace elements in the ocean. Trends Anal. Chem., 30(8), 1291-1307. https://doi.org/10.1016/j.trac.2011.03.006.
Sohrin, Y., Isshiki, K., Kuwamoto, T., Nakayama, E., 1987. Tungsten in north Pacific waters. Mar. Chem., 22(1), 95-103. https://doi.org/10.1016/0304-4203(87)90051-x.
Sohrin, Y., Matsui, M., Nakayama, E., 1999. Contrasting behavior of tungsten and molybdenum in the Okinawa Trough, the East China Sea and the Yellow Sea. Geochim. Cosmochim. Acta, 63(19-20), 3457-3466. https://doi.org/10.1016/s0016-7037(99)00273-2.
Takano, S. et al., 2017. A simple and rapid method for isotopic analysis of nickel, copper, and zinc in seawater using chelating extraction and anion exchange. Anal. Chim. Acta, 967, 1-11. https://doi.org/10.1016/j.aca.2017.03.010.
Takano, S., Tanimizu, M., Hirata, T., Sohrin, Y., 2014. Isotopic constraints on biogeochemical

cycling of copper in the ocean. Nat. Commun., 5, 5663. https://doi.org/10.1038/ncomms6663.

Tanaka, Y., Tsujisaka, M., Zheng, L., Takano, S., Sohrin, Y., 2019. Application of NOBIAS Chelate-PA 1 resin to the determination of zirconium, niobium, hafnium, and tantalum in seawater. Anal. Sci., 35(9), 1015-1020. https://doi.org/10.2116/analsci.19P069.

Thoby, M. et al., 2019. Global importance of oxic molybdenum sinks prior to 2.6 Ga revealed by the Mo isotope composition of Precambrian carbonates. Geology, 47(6), 559-562. https://doi.org/10.1130/G45706.1.

Tsujisaka, M., Nishida, S., Takano, S., Murayama, M., Sohrin, Y., in press. Constraints on redox conditions in the Japan Sea in the last 47,000 years based on Mo and W as paleoceanographic proxies. Geochem. J.

Tsujisaka, M., Takano, S., Murayama, M., Sohrin, Y., 2019. Precise analysis of the concentrations and isotopic compositions of molybdenum and tungsten in geochemical reference materials. Anal. Chim. Acta, 1091, 146-159. https://doi.org/10.1016/j.aca.2019.09.003.

Wang, Z. et al., 2019. Biologically controlled Mo isotope fractionation in coral reef systems. Geochim. Cosmochim. Acta, 262, 128-142. https://doi.org/10.1016/j.gca.2019.07.037.

Wu, F. et al., 2019. Vanadium isotope composition of seawater. Geochim. Cosmochim. Acta, 244, 403-415. https://doi.org/10.1016/j.gca.2018.10.010.

Zhang, R. et al., 2019. Determination of the isotopic composition of tungsten using MC-ICP-MS. Anal. Chim. Acta, 1089, 19-24. https://doi.org/10.1016/j.aca.2019.08.029.

Zhao, P.-P. et al., 2016. Molybdenum mass fractions and isotopic compositions of international geological reference materials. Geostand. Geoanal. Res., 40(2), 217-226. https://doi.org/10.1111/j.1751-908X.2015.00373.x.

Zimmermann, B. et al., 2009. The hafnium isotope composition of Pacific Ocean water. Geochim. Cosmochim. Acta, 73(1), 91-101. https://doi.org/10.1016/j.gca.2008.09.033.

Zurbrick, C.M. et al., 2018. Dissolved Pb and Pb isotopes in the North Atlantic from the GEOVIDE transect (GEOTRACES GA-01) and their decadal evolution. Biogeosciences, 15(16), 4995-5014. https://doi.org/10.5194/bg-15-4995-2018.